Quantification and Localization of Phosphorylated Myosin I Isoforms in *Acanthamoeba castellanii*

Ivan C. Baines, Angela Corigliano-Murphy, and Edward D. Korn

Laboratory of Cell Biology, National Heart, Lung, and Blood Institute, National Institutes of Health, Bethesda, Maryland 20892

Abstract. The actin-activated Mg^{2+}-ATPase activities of the three myosin I isoforms in *Acanthamoeba castellanii* are significantly expressed only after phosphorylation of a single site in the myosin I heavy chain. Synthetic phosphorylated and unphosphorylated peptides corresponding to the phosphorylation site sequences, which differ for the three myosin I isoforms, were used to raise isoform-specific antibodies that recognized only the phosphorylated myosin I or the total myosin I isoform (phosphorylated and unphosphorylated), respectively. With these antisera, the amounts of total and phosphorylated isoform were quantified, the phosphomyosin I isoforms localized, and the compartmental distribution of the phosphomyosin isoforms determined.

Myosin IA, which was almost entirely in the actin-rich cortex, was 70–100% phosphorylated and particularly enriched under phagocytic cups. Myosins IB and IC were predominantly associated with plasma membranes and large vacuole membranes, where they were only 10–20% phosphorylated, whereas cytoplasmic myosins IB and IC, like cytoplasmic myosin IA, were mostly phosphorylated (60–100%). Moreover, phosphomyosin IB was concentrated in actively motile regions of the plasma membrane. More than 20-fold more phosphomyosin IC and 10-fold more F-actin were associated with the membranes of contracting contractile vacuoles (CV) than of filling CVs. As the total amount of CV-associated myosin IC remained constant, it must be phosphorylated at the start of CV contraction. These data extend previous proposals for the specific functions of myosin I isozymes in *Acanthamoeba* (Baines, I. C., H. Brzeska, and E. D. Korn. 1992. *J. Cell Biol.* 119:1193–1203): phosphomyosin IA in phagocytosis, phosphomyosin IB in phagocytosis and pinocytosis, and phosphomyosin IC in contraction of the CV.

LOCALIZATION studies have demonstrated the association of myosin I with membranes in many cell types. In *Acanthamoeba castellanii* myosin I is associated with the plasma membrane (4, 6, 21, 34, 40), the contractile vacuole (CV)[1] (4, 40), digestive vacuole membranes and small cytoplasmic vesicles (6, 40). In *Dictyostelium discoideum*, myosin I is localized to the leading edge of streaming polarized cells whereas conventional myosin II is localized to the posterior region of the same cells (20). In mammalian cell lines and tissues, myosin I has been observed mainly associated with cytoplasmic vesicles or particles (3, 15, 16, 33, 39) and/or the periphery of stationary cells or the leading edge of polarized cells (12, 39). Inferred functions from these localization studies include roles in cell locomotion, phagocytosis, pinocytosis, vesicle transport, CV cycling, dendrite outgrowth, linkage of the plasma membrane to underlying actin bundles and cortical contractility (10, 17, 23, 37). Inferring function from localization is hazardous, however, when it is not known whether a given protein is active in a particular compartment or retained there for other purposes (e.g., storage or transport). For example, brush border myosin I on golgi-derived enterocyte vesicles is probably a passenger on these vesicles (rather than the motor), which are most likely transported to the base of the microvillus by dynein along microtubules (18).

The three myosin isoforms of *Acanthamoeba castellanii* have been well characterized biochemically. Each has a subfragment 1-like domain characteristic of all myosins at the NH_2 terminus of their single heavy chain and a unique COOH-terminal tail with a site that mediates binding of myosin I to membranes (1, 34) or anionic phospholipids (1, 13, 26). The tail also contains a second actin-binding site which is ATP-insensitive (see reference 22 for discussion of tail domains). For maximal expression of actin-activated Mg^{2+}-ATPase activity in vitro (2, 32), the heavy chain must be phosphorylated on a threonine (myosin IA) or serine residue (myosin IB and IC) located between the ATP- and actin-binding sites in the S1-like domain (~38-kD from the NH_2 terminus [8]). By virtue of the binding sites in the tail, the monomeric myosin I isozymes can cross-link actin filaments to membranes or to other actin-

Address all correspondence to Ivan C. Baines, Laboratory of Cell Biology, NHLBI, NIH, Bldg. 3, Rm B1-22, Bethesda, MD 20892. Tel.: (301)496-1616. Fax: (301)402-1519.

1. *Abbreviation used in this paper*: CV, contractile vacuole.

filaments in vitro, and potentially in vivo, but there is little direct information on the functions of any of the *Acanthamoeba* myosin I isoforms.

We previously found by quantitative immunolocalization studies that myosin IA is predominantly localized to the actin-rich cortex below the plasma membrane and is associated with small cytoplasmic vesicles, that myosin IB is predominantly associated with the plasma membrane and the membranes of large cytoplasmic vacuoles, and that myosin IC shares the localization of myosin IB, except that only myosin IC is associated with the CV membrane (4, 6). These immunolocalization studies utilized isoform-specific antibodies that recognized both the unphosphorylated and phosphorylated states of the myosin I. Because the actin-activated Mg^{2+}-ATPase activity of the unphosphorylated myosin I isoforms is very much lower than that of the phosphorylated isoforms, we thought the specific localizations of the latter might provide better insights into the motile functions of each isoform. We now report the results of such experiments utilizing antibodies specific for the phosphorylated state of each *Acanthamoeba* myosin I isoform.

Materials and Methods

Cell Cultures

Acanthamoeba castellanii (Neff strain) were grown either in 1-l culture flasks to a density of 10^6 cell/ml, as described by Pollard and Korn (35), or on a glass substrate in 8-chamber Lab-Tek tissue culture slides (Nunc, Inc., Naperville, IL). Cells grown in contact with a substrate were much flatter than cells grown in suspension thus improving the resolution obtainable by immunofluorescence microscopy.

Purification of Enzymes

Myosins IA, IB, and IC and myosin I heavy chain kinase were purified by the methods described by Lynch et al. (31). The myosins (~1.3 μM) were phosphorylated to the maximal level, 1 mol/mol, by incubation for 40 min at 30°C in 500 μl of phosphorylation buffer (2.5 mM ATP, 3.5 mM $MgCl_2$, 2 mM EGTA, 50 mM imidazole-HCl, pH 7.0) containing 60 nM myosin I heavy chain kinase that had been activated by autophosphorylation by incubation for 15 min at 30°C in phosphorylation buffer containing 0.5 mM phosphatidylserine (9).

Synthesis of Phosphopeptides

Four phosphopeptides were synthesized (the * identifies the phosphorylated amino acid): MIAP = Ala-Gly-Thr*-Thr-Tyr-Ala-Leu-Asn-Leu-Asn-Lys-Met-Gln-Ala, which corresponds to the phosphorylation site of myosin IA (8); MIAP-KK = MIAP with the additional NH_2-terminal sequence Cys-Lys-Lys-, which is not in the myosin IA sequence, and a COOH-terminal Ile, which is in the myosin IA sequence; MIBP = Ala-Lys-Lys-Met-Ser*-Thr-Tyr-Asn-Val-Pro-Gln-Asn-Val-Glu-Gln-Ala, the phosphorylation site of myosin IB (8); MICP = Gly-Arg-Ser-Ser*-Val-Tyr-Ser-Abu-Pro-Gln-Asp-Pro-Leu-Gly-Ala, the phosphorylation site of myosin IC with Abu (α-aminobutyric acid) isosterically substituted for Cys at position 8. MIAP-KK was synthesized because MIAP was insoluble in the conditions used to conjugate the peptide to hemocyanin; the two Lys residues increased solubility and the Cys residue facilitated conjugation.

Full details of the peptide synthesis, purification, analysis and conjugation to hemocyanin will be published elsewhere (Corigliano-Murphy, A., I. C. Baines, and E. D. Korn, manuscript in preparation). Briefly, peptides were synthesized on a peptide synthesizer (430A; Applied Biosystems) by the FastMoc™ coupling protocol (manufacturers instructions) until the residue immediately COOH-terminal to the phosphorylated residue had been coupled. The remainder of the synthesis was performed manually in a 40-ml vessel mounted on a Milligan 504 shaker with 2(1H-benzotriazol-1-yl)-1,1,3,3,-tetramethyluronium hexafluorophosphate, 1-hydroxybenzotriazole and *N,N*,-diisopropylethylamine to mediate coupling. Molar excesses were as follows: 9-fluorenylmethoxycarbonyl amino acid (threefold), 2(1H-benzotriazol-1-yl)-1,1,3,3,-tetramethyluronium hexafluorophosphate (threefold), *N,N*,-diisopropylethylamine (sixfold). The NH_2-terminal amino acid was t-butyloxy carbonyl-protected. After washing and drying under vacuum, half the peptide was transferred to an 8-ml vessel for phosphorylation whereas the rest was subjected to acidolytic cleavage (this unphosphorylated peptide was used to raise antisera). The peptides were phosphorylated with a 20–30-fold molar excess of di-t-butyl-*N,N*-diisopropyl phosphoramidite and a 50–90-fold excess of tetrazole in dry dimethylacetamide. The mixture was blanketed with argon, shaken for 1 h, filtered and then washed with dimethylacetamide. After oxidation with a 20-fold molar excess of t-butyl hydroperoxide in dimethylacetamide for 1 h, the phosphopeptides were filtered, washed sequentially with dimethylacetamide, methanol and methylene chloride, dried under vacuum, and cleaved from the resin with reagent "K" (82.5% trifluoroacetic acid, 5% H_20, 5% phenol, 5% thioanisole, 2.5% ethanedithiol) for 1.5 h. The phosphopeptides were again filtered, washed, and vacuum-dried before partial purification on Sephadex G-25 and further purification by semi-preparative HPLC on either a Vydac C-18 reversed-phase column (1 × 25 cm) for MIAP-KK or a Vydac "pH stable" C-8 reversed-phase column (1 × 25 cm) for MIBP and MICP. Purity was established by analytical HPLC, amino acid analysis following partial and complete hydrolysis, mass spectroscopy and [^{31}P] NMR.

Polyclonal Antibodies

MIAP-KK was conjugated to maleimide-activated keyhole limpet hemocyanin (Pierce Chem. Co., Rockford, IL) according to the manufacturers instructions. MIBP and MICP were conjugated to keyhole limpet hemocyanin (Pierce) by 1-ethyl-3-(3-dimethylaminopropyl) carbodiimide hydrochloride and glutaraldehyde (two-step protocol), respectively, according to Harlow and Lane (24). The conjugated peptides were emulsified with Freunds complete adjuvant (1:1, vol/vol; Difco Laboratories, Detroit, Michigan) before immunization. Female New Zealand white rabbits were primed at the age of 6 mo and received three additional boosts with at least 4-wk intervals between injections. The antisera were collected 10–12 d after the final immunization. Antisera were also raised against all three unphosphorylated peptides (MIA-KK, MIB, and MIC) conjugated to hemocyanin exactly as described for the corresponding phosphopeptide.

Immunolocalization

Cells were fixed and permeabilized according to two distinct protocols (4, 5, 28): (*a*) fixation by 3% formaldehyde and 0.05% glutaraldehyde in growth medium for 45 min at room temperature followed by permeabilization with 100% acetone at −20°C for 30 s; (*b*) simultaneous fixation and permeabilization by immersion in 1% formalin in methanol at −15°C for 5 min (19). The second procedure was used only for indirect immunofluorescence since morphological preservation was too poor for immunogold EM. In both procedures, cells were washed in PBS, pH 7.4, after fixation and after permeabilization and treated with 1 mg/ml of sodium borohydride in PBS for 20 min to reduce free aldehydes. To block nonspecific binding of antibodies, cells were incubated in 1.0% BSA, 50 mM L-lysine and 0.01% sodium ethylmercurithiosalicylate (Thimerosal; Fluka Chemical Corp., Ronkonkoma, NY) in PBS, pH 7.4. Cells were incubated with the primary antibodies (diluted 1:50 in blocking buffer for indirect immunofluorescence and 1:20 for immunogold cytochemistry) and secondary antibodies (diluted 1:50 in blocking buffer for indirect immunofluorescence and 1:2 for immunogold cytochemistry) with five washes with PBS between incubations. To localize F-actin, cells were incubated with either rhodamine phalloidin (Molecular Probes, Inc., Eugene, OR), for fluorescence microscopy, or with biotin-labeled phalloidin (Molecular Probes, Inc.) followed by streptavidin-ferritin (Calbiochem Corp., La Jolla, CA), according to the manufacturer's recommendations, for EM.

Cells labeled with fluorescent probes were mounted in fluorescent mounting medium (Kirkegaard & Perry Labs., Inc., Gaithersburg, MD) and were viewed either by conventional epifluorescent optics with a Zeiss Axioplan microscope equipped with a 40× Neofluor objective or by laser-scanning confocal microscopy with a Zeiss Axiovert 135 inverted microscope and Zeiss LSM 410 confocal attachment (Carl Zeiss, Inc., Thornwood, NY). Cells labeled with gold or ferritin were fixed, post-fixed, dehydrated, embedded, and sectioned for EM, and then viewed with a Philips LS410 electron microscope, as previously described (4). For each antibody, ~20 images (at 17,700×) of single transverse sections passing through the nucleus were collected for each of five different cells. Membrane lengths and cytoplasmic areas were measured with NIH Image™

(National Institutes of Health, Bethesda, MD). Gold particles were counted and the percent partitioning of each myosin I isoform between cellular compartments was calculated as described previously (4, 6).

Quantification

Known amounts of unphosphorylated and phosphorylated myosins IA, IB, and IC, and whole cell lysates were electrophoresed on 7.5% polyacrylamide gels (30), electroblotted onto nitrocellulose according to the manufacturers instructions (Milliblot SDE Transfer System; Millipore Corporation, Bedford, MA), and immunoblotted (38). The myosins were quantified by ECL using antisera raised against the unphosphorylated peptides to determine the amount of total myosin (phosphorylated plus unphosphorylated) and the antisera raised against the phosphopeptides to determine the amount of the phosphorylated isozymes. To minimize the possibility of changes in the state of phosphorylation of the myosins, cells suspended in growth medium ($\sim 1 \times 10^7$ cell/ml) were rapidly lysed in 20% SDS, 1 μM okadaic acid, and 1 mM PMSF. The lysates were adjusted to final concentrations of 2.3% SDS, 5% 2-mercaptoethanol, 10% glycerol, and 0.0625 M Tris-HCl, pH 6.8, for SDS-PAGE. Because the protein concentrations of the lysates were only ~1–5 μg/ml, a maximum of only 40–200 ng of lysate protein could be loaded in each gel lane and, therefore, an excess of antibodies was used to maximize the ECL signal. ECL was performed with an Amersham kit (Amersham Corporation, Arlington Heights, IL) according to the manufacturers instructions and the ECL autoradiograms were scanned with a UltroScan XL (Pharmacia LKB Biotechnology, Piscataway, NJ). Because the assay was linear over only a narrow range of protein concentrations, it was necessary to analyze each sample twice, first with a standard curve ranging from 1 pg to 300 ng of myosin I per lane to determine the approximate amount of myosin in the sample and then with a standard curve expanded over the relevant range to obtain more accurate data.

Other Materials

FITC-conjugated goat anti–rabbit IgG and horseradish peroxidase-conjugated goat anti–rabbit IgG were obtained from Boehringer Mannheim Corp. (Indianapolis, IN). Goat anti–rabbit IgG antibodies conjugated to 5-nm gold particles were obtained from British BioCell International (distributed by Ted Pella, Redding, CA). Glutaraldehyde was from Ted Pella and paraformaldehyde from Fluka Chem. Corp. (Ronkonkoma, NY). All other chemicals were reagent grade.

Results

Antibody Characterization

Anti-phosphomyosin IA and anti-phosphomyosin IB were isotype specific showing no cross-reactivity with either of the other two phosphomyosin I isoenzymes or any of the three unphosphorylated myosins (Fig. 1, *A* and *B*). On immunoblots probed by the ECL technique, anti-phosphomyosin IA detected 1 pg of phosphomyosin IA at dilutions up to 1:800 (Fig. 1 *A*, *g*) and anti-phosphomyosin IB detected 10 pg of phosphomyosin IB at dilutions up to 1:400 (Fig. 1 *B*, *g*). Anti-phosphomyosin IC, on the other hand, recognized both phosphomyosin IC and phosphomyosin IB but it did not react with phosphomyosin IA or any of the unphosphorylated myosins (Fig. 1 *C*); 1 pg of phosphomyosin IC and phosphomyosin IB were detected with equal sensitivity at antisera dilutions up to 1:500 (Fig. 1 *C*, *g*).

On immunoblots of total cell lysates, anti-phosphomyosin IA produced only a single band that corresponded precisely to the position of phosphomyosin IA (Fig. 1 *h*) and anti-phosphomyosin IB produced a single band corresponding to the position of phosphomyosin IB (Fig. 1 *i*). Anti-phosphomyosin IC detected a single band (Fig. 1 *j*) that corresponded to the position of phosphomyosin IC (myosins IB and IC were not resolved on these immunoblots). Preimmune sera for all three antibodies recognized none of the purified myosin I isoforms (phosphorylated or unphosphorylated) and no proteins in the total cell lysates (data not shown). The antisera raised against the three unphosphorylated peptides were isoform specific but recognized unphosphorylated and phosphorylated myosin I with equal sensitivity (data not shown).

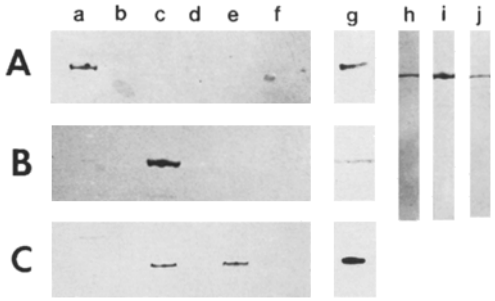

Figure 1. Characterization of antibody specificity by immunoblotting. (*A*, lanes *a–g* and *h*) Anti-phosphomyosin IA raised against MIAP-KK (see Materials and Methods). (*B*, lanes *a–g* and *i*) Anti-phosphomyosin IB raised against MIBP. (*C*, lanes *a–g* and *j*) Anti-phosphomyosin IC raised against MICP. Lanes *a–f* in all three panels contained the following: (*a*) 0.3 μg phosphomyosin IA; (*b*) 0.3 μg unphosphorylated myosin IA; (*c*) 0.3 μg phosphomyosin IB; (*d*) 0.3 μg unphosphorylated myosin IB; (*e*) 0.3 μg phosphomyosin IC; (*f*) 0.3 μg unphosphorylated myosin IC. Lanes *h–j* each contained 40 μg of whole cell lysate. Anti-phosphomyosin IA recognized only phosphomyosin IA (*A*) and a single band in whole cell lysates that co-migrated with phosphomyosin IA (lane *h*); anti-phosphomyosin IB recognized only phosphomyosin IB (*B*) and a single band in whole cell lysates that comigrated with myosin IB (lane *i*); anti-phosphomyosin IC recognized phosphomyosin IB and IC equally well and detected a single band (phosphomyosin IB and IC were not resolved on these immunoblots) in whole cell lysates that comigrated with phosphomyosin IC (lane *j*). Primary antibodies in lanes *a-f* and *h-j* were used after a 1:800 dilution. By ECL, a 1:800 dilution of anti-phosphomyosin IA detected 1 pg of phosphomyosin IA (*A*, lane *g*); a 1:400 dilution of anti-phosphomyosin IB detected 10 pg of phosphomyosin IB (*B*, lane *g*); a 1:500 dilution of anti-phosphomyosin IC detected 1 pg of phosphomyosin IC (*C*, lane *g*). All primary antibodies were detected with anti-rabbit IgG conjugated to horseradish peroxidase and immunoblots were developed by either color reaction (hydrogen peroxide and 4-chloronaphthol; lanes *a–f* and *h–j*) or ECL (lane *g*).

Localization by Indirect Immunofluorescence

Cells were treated in three different ways before fixation to investigate the possible involvement of phosphorylated myosins I in different motile activities. Incubation for 30 min in 50 mM NaCl generated well-polarized highly motile cells; incubation in hypotonic solution (10 mM NaCl) resulted in well defined CVs; incubation for 5 min in growth medium containing lipid-extracted yeast (1 mg or 2.2×10^7 yeast/ml) generated cells with well-defined phagocytic cups and nascent phagosomes.

The immunofluorescence staining patterns obtained with the antibodies that recognized either total myosin IA (Fig. 2, *a–c*) or phosphomyosin IA (Fig. 2, *d–f*) were essentially indistinguishable. As had previously been observed for total myosin IA (6), phosphomyosin IA (Fig. 2

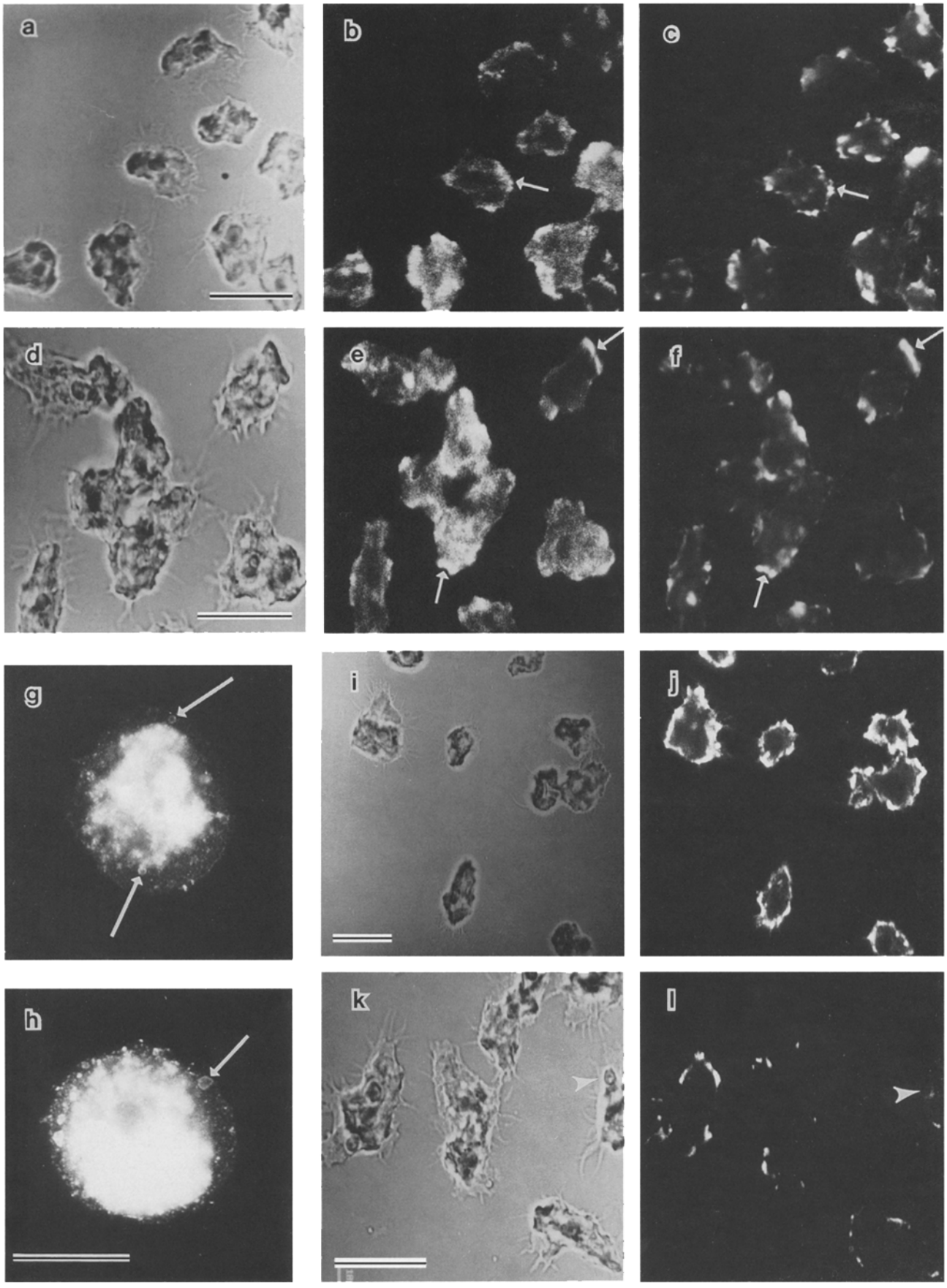
a
b
c
d
e
f
g
i
j
h
k
l

e) was concentrated in specific actin-rich regions (Fig. 2 *f*, *arrows*) of the cortex. When cells were fixed in 1% formalin in methanol after a short incubation in hypotonic buffer, cortical F-actin was lost which allowed small cortical vesicles with associated myosin IA to be clearly visualized with both antisera (Fig. 2, *g* and *h*). In contrast to myosin IA, the immunofluorescence images obtained with anti-phosphomyosin IB (Fig. 2, *k* and *l*) were distinctly different from those obtained with antisera that recognized total myosin IB (Fig. 2, *i* and *j*; and reference 6). Whereas total myosin IB was uniformly distributed around the cell perimeter (Fig. 3 *j*), phosphomyosin IB was concentrated in highly localized regions of the cortex and plasma membrane (Fig. 3 *l*).

In polarized migrating cells, phosphomyosin IA and F-actin were concentrated in the cortex at the front of the cell and in the cortex of the posterior uroid (Fig. 3 *a*), whereas phosphomyosin IB was associated with the plasma membrane of the leading edge of pseudopodia (Fig. 3 *b*). During phagocytosis, phosphomyosin IA was concentrated in the cortex of the phagocytic cup (Fig. 3 *c*) whereas phosphomyosin IB was associated with the membrane of nascent phagocytic cups (Fig. 3 *d*, *arrow*). Phosphomyosin IB was also concentrated in protrusions such as acanthapods (Fig. 3 *e*) and showed a punctate staining pattern in ultra-thin lamellipodia (Fig. 3 *f*). As the anti-phosphomyosin IC also recognized phosphomyosin IB, it could not be determined how much of the immunofluorescence of the plasma membrane (Fig. 4, *e* and *f*) and of a subset of digestive vacuoles observed with this antibody (data not shown) was due to the presence of phosphomyosin IC. However, as the CV membrane does not contain any myosin IB (6), the fluorescence associated with this organelle (Fig. 4, *e* and *f*) must have been due to phosphomyosin IC. CVs were stained differently by the antibodies that recognized total myosin IC and those that recognized only phosphomyosin IC. Whereas the antibody recognizing total myosin IC labeled a CV in every cell (Fig. 4, *a* and *d*), the antibody specific for phosphomyosin IC detected only those CVs that were either larger than average (Fig. 4, *b* and *e*, *arrow*) or adjacent to the plasma membrane (Fig. 4, *c* and *f*, *arrows*). These results suggest that phosphomyosin IC occurs only in full CVs at the start of systole or in vacuoles that are actively contracting.

Localization by Immunogold EM

The immunofluorescence intensities are proportional to the relative concentrations, not the relative amounts, of a myosin I isoform in each cell compartment and also depend on the particular contrast and brightness settings used for microscopy and photomicrography. Quantitative data on the isoform composition of each cell compartment can be obtained, however, by immunogold EM. First, the percent distribution of each myosin I isoform (total and phosphorylated) in each cellular compartment is determined from the distribution of gold particles. From these data and the absolute amount of each isoform in the cell, determined independently, the total and phosphorylated myosin I isoform composition of each compartment can be readily calculated (for details, see reference 6).

The total amount of myosin I, as determined by the ECL method (Table I), was ~50% greater than had been previously found by immunoprecipitation (6). The ECL data are probably more accurate because small amounts of myosin were likely to have been lost at each of the multiple washing steps employed during quantitative immunoprecipitation. In agreement with the previous results, myosins IA, IB, and IC accounted for ~10, 70, and 20% of the total myosin I pool, respectively. Although total myosin I was approximately equally distributed between the three major compartments: plasma membrane, cytoplasm, and large vacuole membranes, the three isoforms were differently distributed: IA was almost exclusively in the cytoplasm, especially in the actin-rich cortex and associated with small vesicles, whereas 80% of IB and 95% of IC were associated with plasma membranes and large vacuole membranes (Table I).

Table I. Amount and Compartmental Distribution of Total Myosin I and Phosphomyosin I Isoforms

	IA	IB	IC	Total
	*ng/10⁶ cells (± standard error)**			
Total myosins				
Total cell	52 ± 14	299 ± 43	82 ± 7	433‡
Plasma membrane	4	117	36	157
Cytoplasm	48	51	5	104
Vacuoles	0	132	40	172
Phosphomyosins				
Total cell	55 ± 7	54 ± 12	18 ± 4	127
Plasma membrane	4	11	10	25
Cytoplasm	50	32	7	89
Vacuoles	1	11	1	13

*Total myosin I and phosphomyosins I isoforms were quantified by ECL in triplicate for each of five different suspension cell cultures. An average value for each culture was calculated (by averaging the triplicate measurements) before averaging the five values so obtained to give means of means (± standard error). Phosphomyosin IC was calculated as the difference in the amount of phosphomyosin I detected by the phosphomyosin IB-specific antibody and the amount detected by the antibody which recognizes both phosphomyosins IB and IC. To determine the amounts of each isoform in each compartment, gold particles were counted in complete transverse sections of five different cells for each antibody and the fractional partitioning of each isoform between compartments was calculated as previously described (5) based on a plasma membrane surface area of 2,590 μm^2, a cytoplasmic volume of 2,540 μm^3, a total surface area of 2,032 μm^2 for the large vacuolar system (7), and a constant section thickness of 75 nm.

‡Equivalent to 1,700,000 molecules/cell.

Figure 2. Localization of phosphomyosin I isoforms by indirect immunofluorescence. (*a–f*) DIC (*a* and *d*) and fluorescence images (*b* and *c*, *e* and *f*) of cells incubated in 50 mM NaCl, fixed by protocol 1 (see Materials and Methods) and stained with either anti-myosin IA and rhodamine-phalloidin (*a–c*) or anti-phosphomyosin IA and rhodamine-phalloidin (*d–f*). Both total myosin IA (*b*) and phosphomyosin IA (*e*) were concentrated in particular regions of the cortex (*arrows*) which also contained F-actin (*c* and *f*). (*g* and *h*) Cells incubated in hypotonic saline (10 mM) were fixed according to protocol 2 (see Materials and Methods) and were stained with either anti-total myosin IA (*g*) or anti-phosphomyosin IA (*h*); arrows indicate cortical vesicles. (*i–l*): DIC (*i* and *k*) and fluorescence (*j* and *l*) images of cells incubated in the presence of yeast, fixed by protocol 1 and stained with either anti-total myosin IB (*i* and *j*) or anti-phosphomyosin IB (*k* and *l*). All panels are confocal images collected at identical contrast and brightness settings except for *g* and *h* which were taken by conventional fluorescence microscopy. Bars: (*a, d, i, k*) 20 μm; (*g* and *h*) 10 μm.

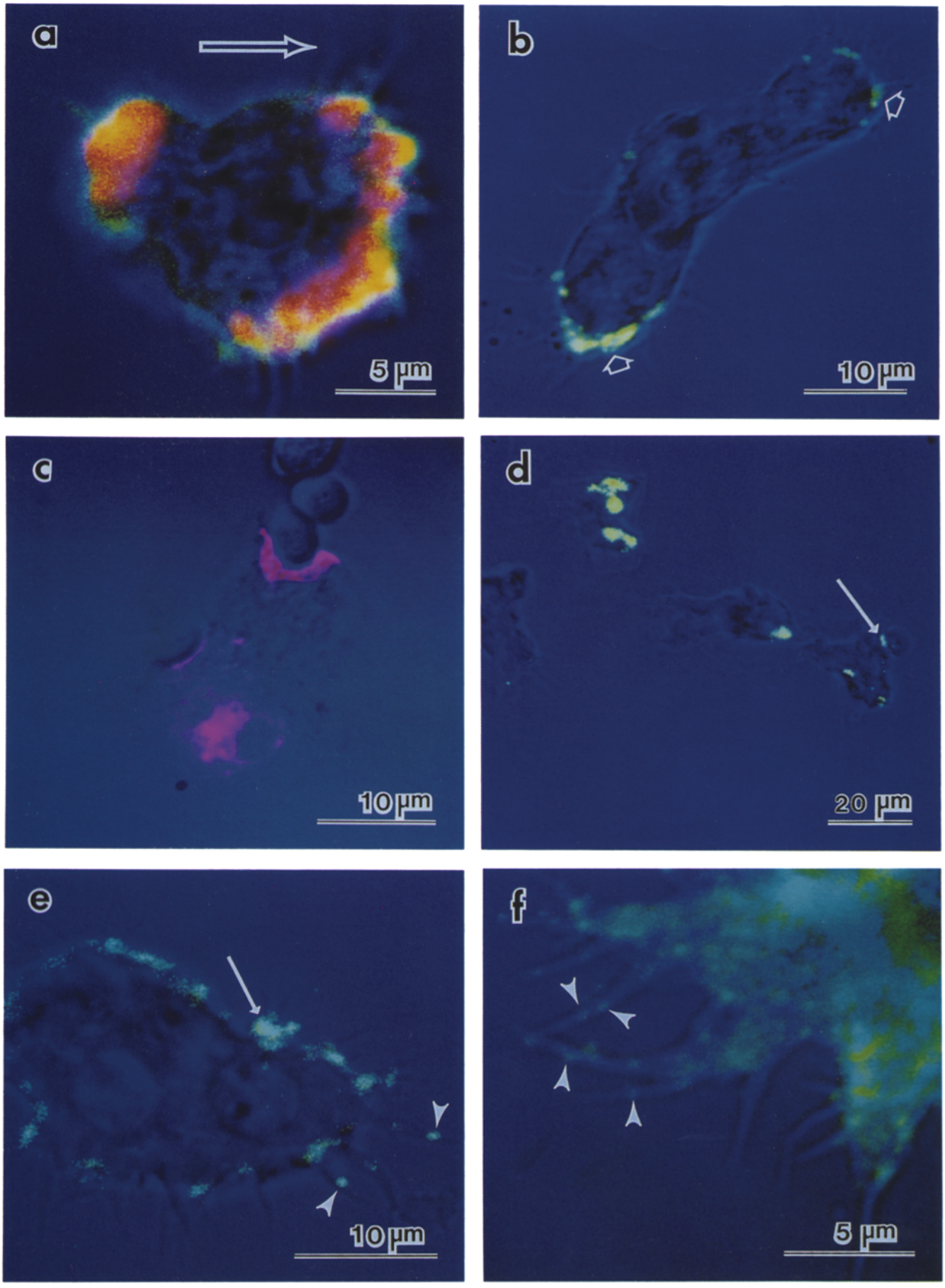
a
5 μm
b
10 μm
c
10 μm
d
20 μm
e
10 μm
f
5 μm

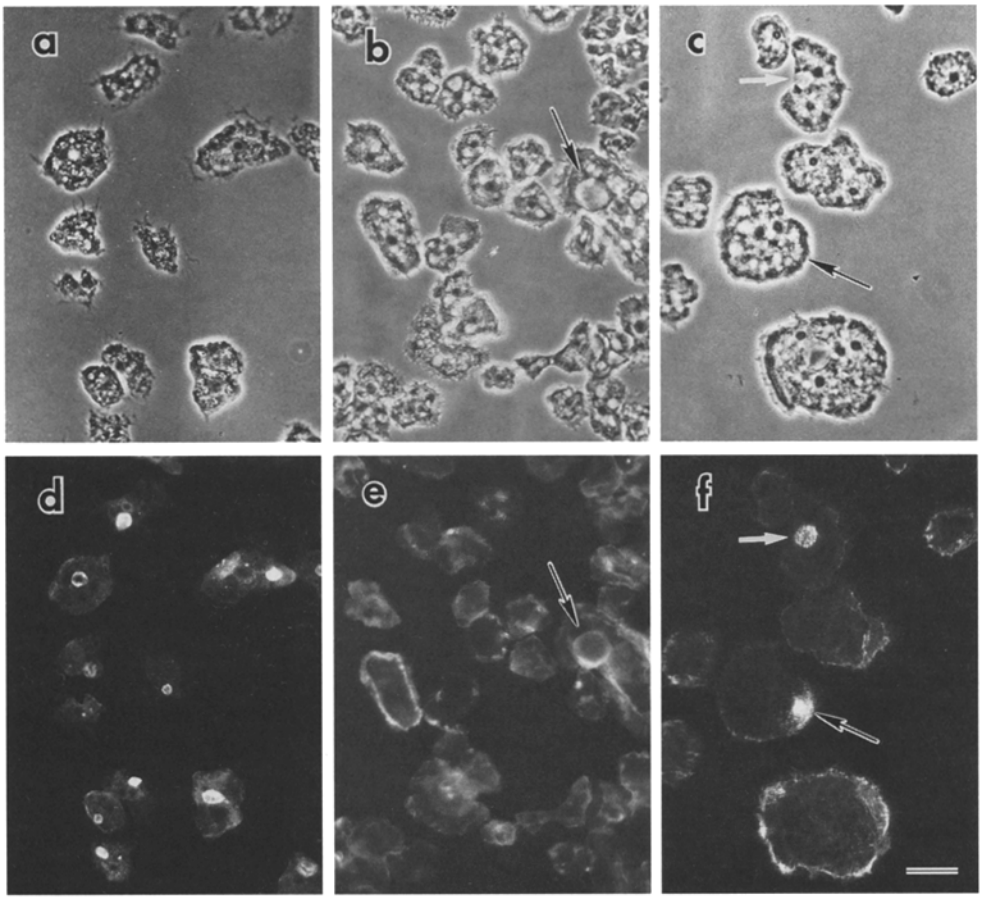

Figure 4. Indirect immunofluorescence of myosin IC and phosphomyosin IC associated with contractile vacuoles. Cells were incubated in hypotonic saline (10 mM NaCl), fixed by protocol 1 and stained with either anti-total myosin IC (*a*, phase contrast; *d*, fluorescence) or anti-phosphomyosin IC (*b* and *c*, phase contrast; *e* and *f*, fluorescence). The arrows in *b* and *e* indicate a larger than average CV; arrows in *c* and *f* indicate CVs closely apposed to the plasma membrane. Bar, 10 μm.

By ECL quantification, ~30% of the total myosin I was phosphorylated (Table I) comprising 70–100% of myosin IA but only 15–18% of myosin IB and 7–22% of myosin IC (range calculated from standard errors). As expected, because most of the myosin IA was phosphorylated, phosphomyosin IA and total myosin IA were similarly partitioned between the plasma membrane, the cell cortex, and in association with membranes of small vesicles and the cytoplasmic surface of the plasma membrane (Fig. 5 *a*, Table I). On the other hand, phosphomyosins IB and IC were distributed differently than total myosin IB and IC with a much higher fraction of the phosphorylated isoforms in the cytoplasm than in the two membrane fractions. In sum, the total cytoplasmic myosin I was ~85% phosphorylated (90% of which was phosphomyosins IA and IB), total plasma membrane-associated myosin I was ~16% phosphorylated (85% of which was phosphomyosins IB and IC) and total large vacuole membrane-associated myosin I was ~7% phosphorylated (95% of which was phosphomyosin IB).

In contrast to the uniform distribution of total myosin IB in the plasma membrane (6), phosphomyosin IB (which was 10% of the total myosin IB) was concentrated in specific regions which, by morphological criteria, corresponded to regions of pinocytosis (Fig. 5 *b*, *arrows*) or phagocytosis (not shown), filopodia (Fig. 6) and pseudopodia (not shown). Phosphomyosin IB was about five times more concentrated in regions of membrane invaginations (Fig. 5 *b*) and protrusions (Fig. 6) than its average concentration for the entire plasma membrane and 10–30 times more concentrated than in some other regions of the plasma membrane (Table II).

Controls for Immunogold EM

A preembedding immunogold staining protocol was used

Figure 3. Laser scanning confocal microscopy of phosphomyosin I in either motile cells (*a* and *b*), phagocytosing cells (*c* and *d*), cells fixed in suspension (*e*) or on a substrate (*f*) and stained with either anti-phosphomyosin IA (*a* and *c*), anti-phosphomyosin IB (*b*, *d–f*), or rhodamine phalloidin (*a*). All images are superimposed DIC (*blue*) and confocal fluorescence (*red* and/or *green*). (*a*) Phosphomyosin IA (*green*) is concentrated at the front and rear of migrating cells where it substantially colocalizes (*yellow*) with F-actin (*red*). The arrow indicates the direction of cell migration. (*b*) Phosphomyosin IB (*green*) is present at the leading edges of pseudopodia (*arrows*). (*c*) During phagocytosis, phosphomyosin IA (*red*) is concentrated in the cortical region surrounding the phagocytic cup. (*d*) During phagocytosis, phosphomyosin IB (*green*) is associated with the plasma membrane at the site of contact between the cell and the particle to be ingested (*arrow*). Phosphomyosin IB (*green*) is concentrated in filopodia (*arrows*) of cells fixed in suspension (*e*) and in ultra-thin lamellipodia of cells fixed on a substrate (*f*). Intense fluorescence bleaches the color-carrying capacity of the photographic paper and, thus, the regions of most intense staining appear white in these photographs.

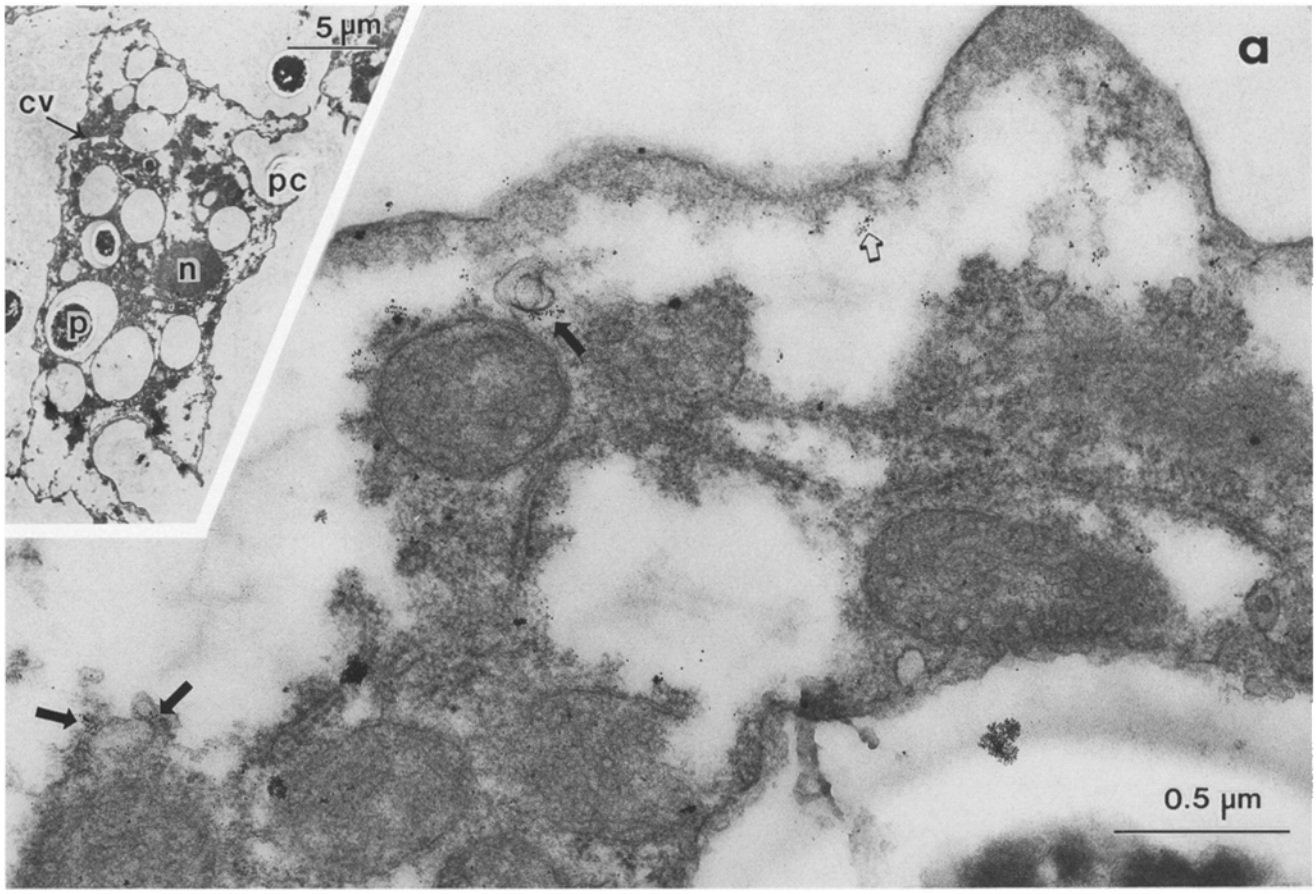
5 μm
cv
pc
n
p
a
0.5 μm

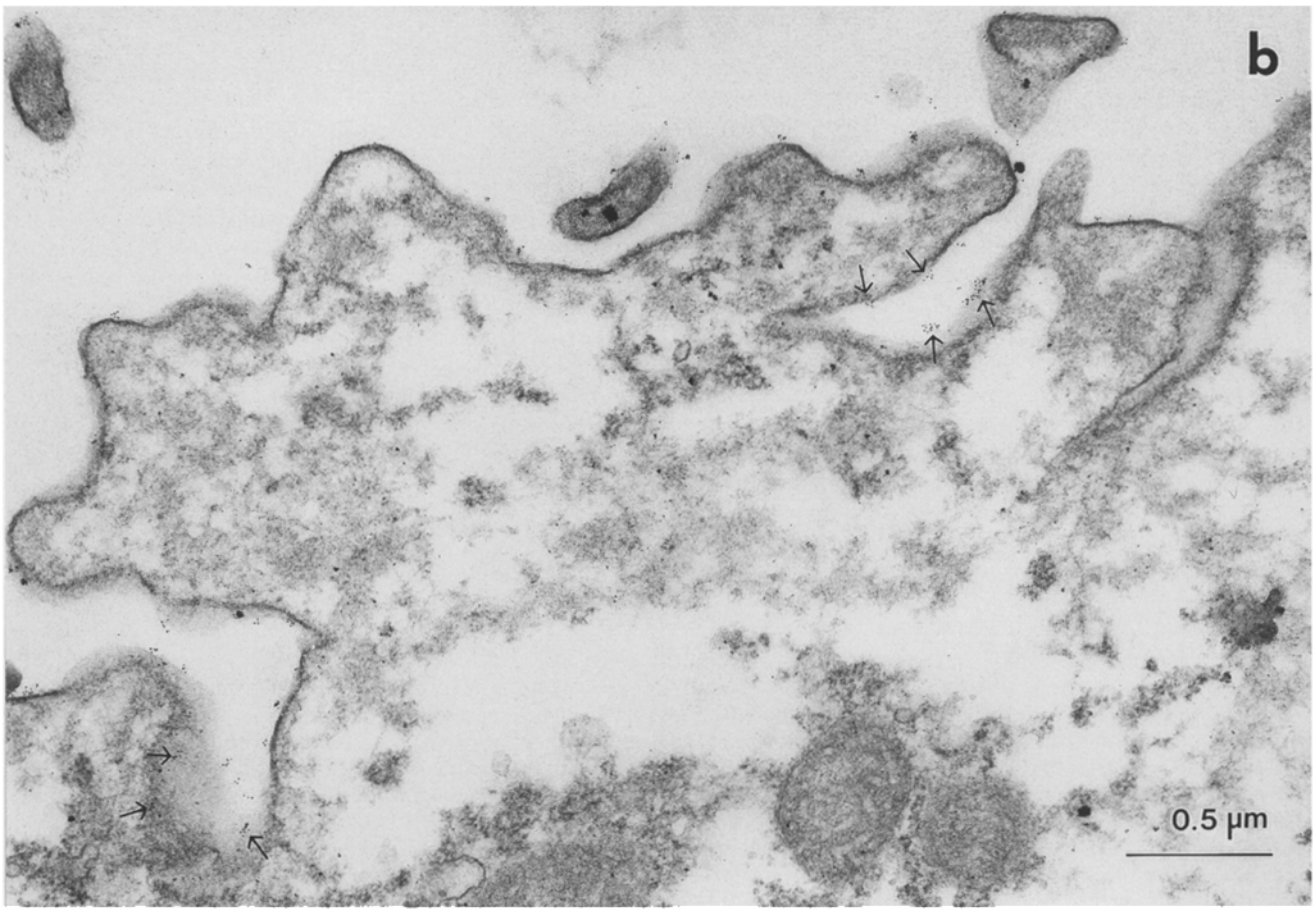
b
0.5 μm

in this study because post-embedding labeling methods provided poor signal to noise ratios. The dilution of the antibodies and number and duration of washes after antibody incubations were such that all background labeling in preimmune serum-treated samples (not shown) was removed and, therefore, all remaining label in the identically treated immune samples was specific for the primary antibodies. The results of immunogold EM were entirely consistent with those obtained by immunofluorescence, with a higher density of gold particles in each location that had been observed by indirect immunofluorescence to have greater fluorescence intensity.

Preembedding immunogold EM requires permeabilization of the cells to allow entry of antibodies. Although permeabilization was performed on cells prefixed with aldehydes, it might still extract or change the location of myosin I isoforms. If extraction occurred equivalently in all cellular compartments, the quantitative percent partitioning data would not be affected. However, preferential extraction of myosin I from one compartment would result in incorrect partitioning data. To try and control for this, two complete cell sections were quantified for each antibody using the light, intermediate and extensive saponin permeabilization protocols described previously (4, 6, 29). Intermediate saponin permeabilization yielded similar results (not shown) to those obtained in the present study on acetone-permeabilized cells. Comparison of the quantification after intermediate permeabilization with that after light and extensive permeabilization indicated that membrane-associated myosin IB and IC were more labile to permeabilization than myosin IB or IC in the cytoplasm or other compartments. Extensive detergent treatment could extract as much as ~50% of the membrane-associated myosin IB and IC. However, any differentially greater extraction of membrane-associated myosins IB and IC that may have occurred in the experiments quantified in Table I would have had little effect on the calculations as 83% of IB and 94% of IC were found to be membrane associated. The different permeabilization procedures had no demonstrable effect on myosin IA.

Some of the plasma membrane myosin IB gold label appears to have a bias to the external surface. Cells that were labeled with antibodies without prior permeabilization showed no gold label on the surface of the cell (results not shown) indicating that myosin IB is not normally exposed on the cell surface. Possible causes of an external bias to plasma membrane gold labeling are discussed elsewhere (4).

Quantification of the Association of Phosphomyosin IC and Actin with CV Membranes

Myosin IC is the only myosin I isoform associated with CV membranes, and an antibody that recognizes total myosin IC (4) labeled CVs equally at all stages of systole and diastole. In contrast, in the present study, phosphomyosin IC was not detected on all CVs (Fig. 4). The CVs that were labeled could be assigned, by morphological criteria, to one of three classes (Fig. 7). Membranes of full CVs (Fig. 8 *b*) had about six times more associated phosphomyosin IC (Table III) and membranes of contracting vacuoles (Fig. 8 *c*) ~20 times more phosphomyosin IC than membranes of filling vacuoles (Fig. 8 *a*). As the amount of phosphomyosin IC associated with the CV membrane changes ~20-fold during the CV cycle while the amount of total myosin IC remains constant, myosin IC must go through a phosphorylation-dephosphorylation cycle while remaining membrane-bound during the functional cycle of the CV.

Table II. Concentration of Phosphomyosin IB in Regions of Plasma Membrane (PM) Activity

	Active PM	Average PM	Minimum PM
	particles/μm (± standard deviation)		
Invaginations	32 ± 8.7 (max 86)	6.8 ± 0.8	2.9 ± 0.5
Protrusions	35 ± 14 (max 77)	7.7 ± 1.6	3.4 ± 1.1

The density of membrane-associated gold particles (all particles falling within a zone extending 10 nm on either side from the middle of the membrane, see reference 5) was quantified for membranes associated with invaginations or protrusions (active PM), the entire plasma membrane (average PM) and regions excluding protrusions or invaginations (minimum PM). For protrusions a membrane length of 5.0 ± 1.1 μm (n = 8) and for invaginations a membrane length of 5.7 ± 1.2 μm (n = 7) was quantified for a minimum of four cells.

Myosins mediate contractile events only when combined with filamentous actin. For this reason, the amount of F-actin associated with the three aforementioned stages of the CV was quantified by biotinylated phalloidin. The pattern (Fig. 8, *d–f*) was similar to that of phosphomyosin IC; the amount of F-actin associated with the CV membrane changed more than 10-fold during the CV cycle (Table III). Both F-actin and phosphomyosin IC were most concentrated when the vacuole was contracting.

Discussion

Phosphorylation of the *Acanthamoeba* myosin I heavy chain is required for maximal expression of actin-activated Mg^{2+}ATPase activity in vitro (2, 32) and, therefore, it is reasonable to assume that actomyosin-dependent motile events in vivo occur in regions of the cell that contain both F-actin and phosphomyosin I. We find that ~30% of the total myosin I is phosphorylated but that the level of phosphorylation varies with the location of the myosin I and is different for each isoform. Thus, cytoplasmic myosin I, which is principally but not exclusively myosin IA, is 60–100% phosphorylated whereas membrane-associated myosin I, which is principally myosin IB and IC, is only 10–20% phosphorylated. Almost all of the myosin IA in the cell is phosphorylated but only 10–20% of myosin IB and IC are phosphorylated.

The phosphomyosin isoforms are also distributed differently within the membrane and cytoplasmic compartments. Phosphomyosin IA and IB are localized to par-

Figure 5. Immunogold EM of phosphomyosin IA and IB. Phosphomyosin IA (*a*) was associated with small vesicles (*a, solid arrows*) and the cortex underlying the plasma membrane (*a, open arrow*). The inset in *a* shows a full transverse section of one of the cells which were quantified for phosphomyosin IA. The clear regions are most likely the result of glycogen extraction. Phosphomyosin IB was concentrated on the membrane of pinocytic invaginations (*b, arrows*). *n*, nucleus; *p*, phagosome; *pc*, phagocytic cup; *cv*, contractile vacuole.

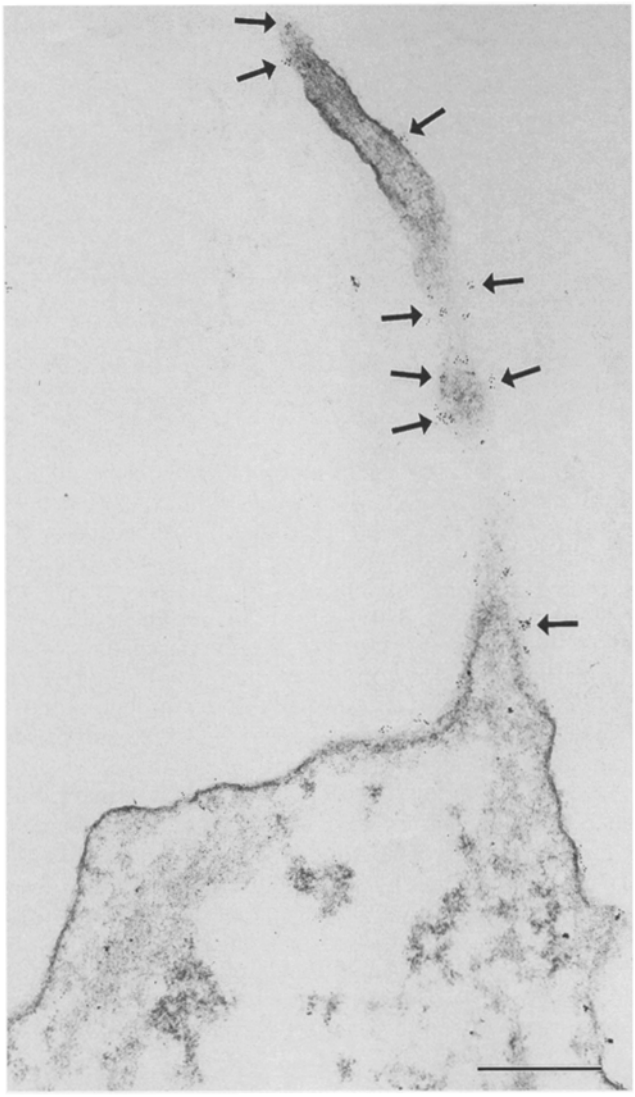

Figure 6. Concentration of phosphomyosin IB on the membranes of protrusions. There are a greater number of gold particles (*arrows*) on the membrane of the protrusion than on the membrane of the cell body on either side of the protrusion. Bar, 0.5 μm.

ticular regions of the cortex, e.g., phosphomyosin IA is concentrated in the sub-plasma membrane, actin-rich cortex especially surrounding phagocytic cups. About 95% of the phosphomyosin associated with the membranes of digestive vacuoles is phosphomyosin IB whereas phosphomyosin IA is the only phosphorylated myosin I associated with small cytoplasmic and cortical vesicles. The CV membrane contains only phosphomyosin IC. Plasma membrane-associated phosphomyosin IB is more than 10-fold concentrated in regions of the plasma membrane engaged in motile activities such as pseudopod extension, filopod formation, or pinocytic invagination.

At any time and place, the concentration of a phosphomyosin I isoform is a consequence of the relative rates of its phosphorylation and dephosphorylation. An increase in the local concentration of one or more phosphomyosins could result from either or both an increase in the total concentration (unphosphorylated and phosphorylated myosin) or an increase in the fraction that is phosphorylated by either specific recruitment of phosphomyosin into that region or an increase in the phosphorylation rate (and/or a decrease in the rate of dephosphorylation). For example, at all times, most of the plasma membrane-associated myosin IB is unphosphorylated and, presumably, inactive. The increase in phosphomyosin IB concentration in the membranes of phagocytic cups could be due to the recruitment of phosphomyosin IB to the region of membrane in contact with the particle to be ingested (6) or a contact-mediated change in the local rate of myosin phosphorylation or dephosphorylation. Both the plasma membrane and cytoplasm contain myosin I heavy chain kinase (28) and activation of either kinase pool in the region of membrane–particle contact could increase the concentration of phosphomyosin IB. However, at least in vitro, kinase associated with plasma membranes is inherently substantially activated (in contrast to soluble kinase that must be activated by autophosphorylation [29]). This raises the possibility that the increase in local concentration of phosphomyosin IB associated with phagocytosis results not from a local activation of kinase but from local facilitation of kinase–myosin contact (or decrease in the rate of phosphomyosin IB dephosphorylation). It is interesting that the concentration of phosphomyosin IB at regions of membrane involved in motile processes, ~200 molecules per μm^2 (calculated from the data in Table II and a plasma membrane area of 2,590 μm^2 [7]), is similar to the K_m for myosin I on the surface of phospholipid vesicles, ~500 molecules per μm^2 (Wang, Z. Y., H. Brzeska, I. C. Baines, and E. D. Korn, manuscript in preparation). However, the phosphorylation of phospholipid-bound myosin I by phospholipid-bound kinase in vitro is largely intervesicular (Wang, Z. Y., H. Brzeska, I. C. Baines, and E. D. Korn, manuscript in preparation) so either there must be significant differences in the interaction of kinase and myosin I in situ if kinase phosphorylates myosin I in the same membrane or membrane-associated myosin IB is principally phosphorylated by soluble autophosphorylated kinase present in the cortex (28).

In contrast to the myosin I in the plasma membrane, most of the cytoplasmic myosin I is phosphorylated and, therefore, presumably always in its active state. This suggests that active cytoplasmic phosphomyosin I might be specifically recruited to regions where it is required rather than locally phosphorylated.

The constant high level of phosphorylation of cortical myosin I suggests that it is involved in maintaining cortical tension, probably by generating force between actin filaments. The increased concentration of cortical myosin I,

Table III. Correlation of CV-associated Phosphomyosin IC and F-actin with the CV Cycle

Cycle stage	Phosphomyosin IC	F-actin
	particles/μm	
Filling	0.5 ± 0.3	7.8 ± 4.0
Full	3.0 ± 1.2	26.4 ± 6.6
Contracting	11.7 ± 5.0	84.4 ± 6.9

Membrane-associated (see Table II for definition) gold particles (phosphomyosin IC) or ferritin (F-actin) were counted in transverse sections of five different CVs at each stage and divided by the total CV membrane length to give the density of labeling.

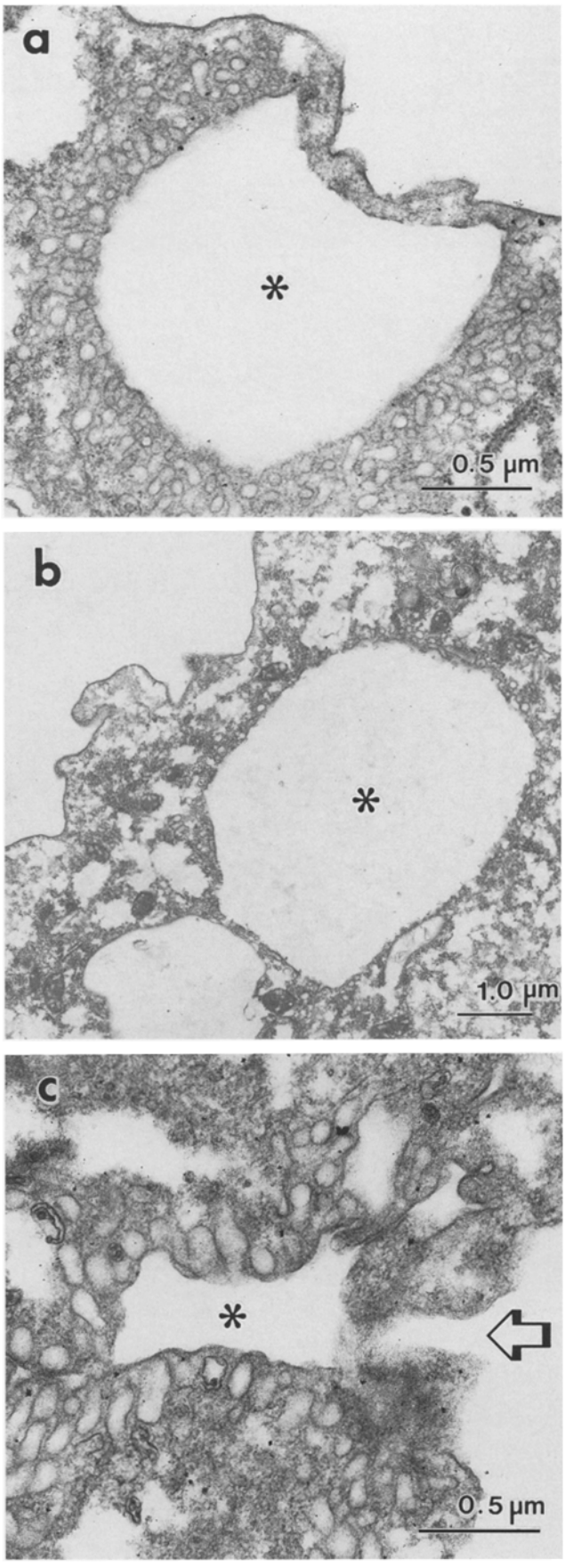

especially myosin IA, around phagocytic cups suggests that it is specifically involved in the movement of cytoplasm into the extending pseudopods, probably by moving actin filaments relative to each other. Phosphomyosin IB, which is enriched in the plasma membrane of phagocytic cups and at the tips of pseudopods (6), would be in a position to link the plasma membrane to the underlying F-actin and, thereby, mediate membrane protrusion during pseudopod extension.

F-actin would be involved in these motile processes as the activator of myosin I ATPase activity and possibly as a sliding filament. The organization of F-actin, as controlled by its interaction with a large family of actin-binding proteins (for reviews see references 25 and 36), might determine whether the actin-based structure were able to contract (11). In addition, the interaction of myosins with F-actin can be regulated by actin-binding proteins (e.g., the tropomyosin–troponin complex in muscle). The observation that myosin IB is excluded from certain actin-rich regions in the cortex (6) whereas phosphomyosin IB is enriched in other specific actin-rich cortical regions (e.g., in the cortex of pseudopodia) is consistent with the existence of such a regulatory system for actomyosin I. Thus, myosin I might be recruited to a particular actin structure or its functional interaction with F-actin might be regulated by one or more sets of actin-binding proteins.

Myosin IC is present at equivalent densities on the CV membrane at all stages of the functional cycle. However, the vacuole-associated myosin IC is phosphorylated only during and immediately preceding vacuole contraction. The association of F-actin with the CV membrane is also coupled to the CV cycle such that the concentration of F-actin increases at the same time as the concentration of phosphomyosin IC. Therefore, F-actin and phosphomyosin IC appear to be temporally and spatially positioned to mediate actomyosin-dependent contraction of the CV. These observations are entirely consistent with earlier work showing that antibodies that block myosin IC phosphorylation and binding of myosin IC to F-actin in vitro inhibit CV function in vivo causing cells subjected to hypotonic media to lyse (14).

In summary, by quantifying and localizing phosphorylated Acanthamoeba myosin I isoforms it has been possible to gain greater insight into the roles of each isoform. Myosin IA is probably primarily involved in small vesicle transport and cortical contraction (which would include maintenance of the structural integrity of the cortex (11, 27), myosin IB in membrane protrusion during phagocytosis and pinocytosis (and possibly in the movement of nascent digestive vacuoles, although the phosphomyosin IB

Figure 7. Classification of different stages of contractile vacuole activity by morphology. CVs were classed as filling (*a*), if the vacuole membrane bulged out from the lumen (concave with respect to lumen) and the vacuole was surrounded by an extensive spongiome; full (*b*), if the vacuole was large, spherical and had a reduced or nonexistent spongiome; or contracting (*c*), if the vacuole membrane bulged into the lumen and there was an opening to the external medium (*arrow*). Partial serial sectioning was necessary to class some vacuoles but only those vacuoles that could be unambiguously classified were used for quantification (Table IV).

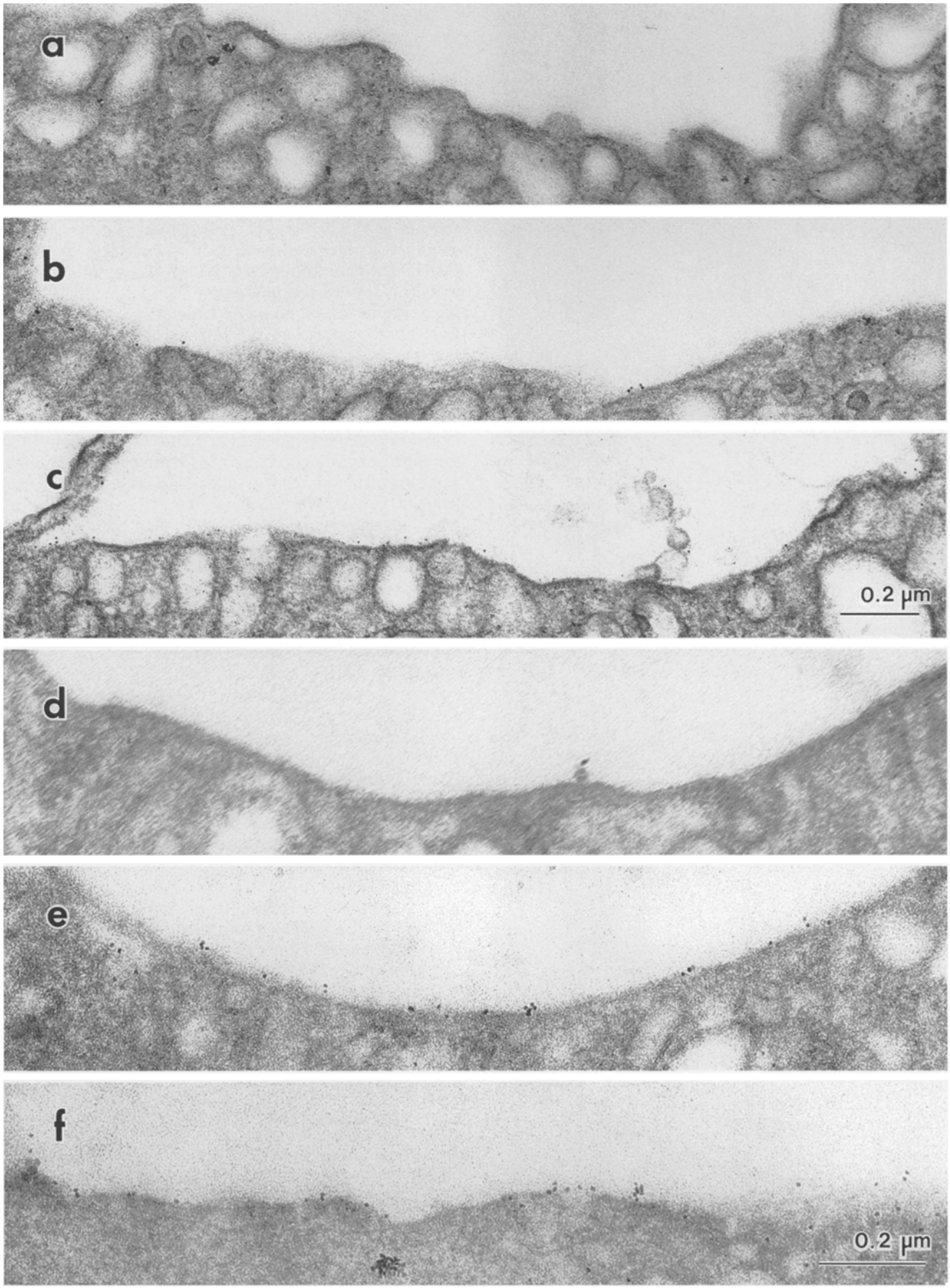

Figure 8. Stage-dependent association of phosphomyosin IC and F-actin with contractile vacuole membranes. Phosphomyosin IC gold label was either absent or scarce on the membranes of filling vacuoles (*a*), was more common on the membranes of full vacuoles (*b*) and was abundant on the membranes of contracting vacuoles (*c*). A similar pattern was observed for F-actin association with filling (*d*), full (*e*), and contracting (*f*) vacuoles.

on the large vacuole membranes might just be a nonfunctional residue from the internalized plasma membrane), and phosphomyosin IC in the contracting stage of the CV cycle.

The authors thank Dr. H. Brzeska for providing myosin I heavy chain kinase and Drs. H. Brzeska, Z. Y. Wang, and K. B. Kwak for assistance in the purification of myosin I isoforms.

Received for publication 10 April 1995 and in revised form 13 April 1995.

References

1. Adams, R. J., and T. D. Pollard. 1989. Binding of myosin I to membrane lipids. *Nature (Lond.).* 340:565–568.
2. Albanesi, J. P., M. Coué, H. Fujisaki, and E. D. Korn. 1985. Effect of actin filament length and filament number concentration on the actin-activated ATPase activity of *Acanthamoeba* myosin I. *J. Biol. Chem.* 260: 13276–13280.
3. Bähler, M., R. Kroschewski, H. Stöffler, and T. Behrmann. 1994. Rat myr 4 defines a novel subclass of myosin I: identification, distribution, localization, and mapping of calmodulin-binding sites with differential calcium sensitivity. *J. Cell Biol.* 126:375–389.
4. Baines, I. C., and E. D. Korn. 1990. Localization of myosin IC and myosin II in *Acanthamoeba castellanii* by indirect immunofluorescence and immunogold electron microscopy. *J. Cell Biol.* 111:1895–1904.
5. Baines, I. C., and E. D. Korn. 1994. *Acanthamoeba castellanii*: a model system for correlative biochemical and cell biological studies. *In* Cell Biology: A Laboratory Handbook. Vol. 1. J. E. Celis, editor. Academic Press, Inc., San Diego, CA. 405–411.
6. Baines, I. C., H. Brzeska, and E. D. Korn. 1992. Differential localization of *Acanthamoeba* myosin I isoforms. *J. Cell Biol.* 119:1193–1203.
7. Bowers, B., T. E. Olszewski, and J. Hyde. 1981. Morphometric analysis of volumes and surface areas in membrane compartments during endocytosis in *Acanthamoeba*. *J. Cell Biol.* 88:509–515.
8. Brzeska, H., T. J. Lynch, B. Martin, and E. D. Korn. 1989. The localization and sequence of the phosphorylation sites of *Acanthamoeba* myosins I. *J. Biol. Chem.* 264:19340–19348.
9. Brzeska, H., T. J. Lynch, and E. D. Korn. 1990. *Acanthamoeba* myosin I heavy chain kinase is activated by phosphatidylserine-enhanced phosphorylation. *J. Biol. Chem.* 265:3591–3594.
10. Cheney, R. E., and M. S. Mooseker. 1992. Unconventional myosins. *Curr. Opin. Cell Biol.* 4:27–35.
11. Condeelis, J. 1993. Life at the leading edge: the formation of cell protrusions. *Annu. Rev. Cell Biol.* 9:411–444.
12. Conrad, P. A., K. A. Giuliano, G. Fisher, K. Collins, P. T. Matsudaira, and D. L. Taylor. 1993. Relative distribution of actin, myosin I, and myosin II during the wound healing response of fibroblasts. *J. Cell Biol.* 120:1381–1391.
13. Doberstein, S. K., and T. D. Pollard. 1992. Localization and specificity of the phospholipid and actin-binding sites on the tail of *Acanthamoeba* myosin IC. *J. Cell Biol.* 117:1241–1249.
14. Doberstein, S. K., I. C. Baines, G. Weigand, E. D. Korn, and T. D. Pollard. 1993. Inhibition of contractile vacuole function *in vivo* by antibodies against myosin-I. *Nature (Lond.).* 365:841–843.
15. Drenckhahn, D., and R. Dermietzel. 1988. Organization of the actin filament cytoskeleton in the intestinal brush border: a quantitative and qualitative immunoelectron microscopy study. *J. Cell Biol.* 107:1037–1048.
16. Fath, K. R., and D. R. Burgess. 1993. Golgi-derived vesicles from developing epithelial cells bind actin filaments and possess myosin-I as a cytoplasmically oriented peripheral membrane protein. *J. Cell Biol.* 120:117–127.
17. Fath, K. R., and D. R. Burgess. 1994. Membrane motility mediated by unconventional myosin. *Curr. Opin. Cell Biol.* 6:131–135.
18. Fath, K. R., G. M. Trimbur, and D. R. Burgess. 1994. Molecular motors are differentially distributed on golgi membranes from polarized epithelial cells. *J. Cell Biol.* 126:661–675.
19. Fukui, Y., S. Yumura, T. K. Yumura, and H. Mori. 1986. Agar overlay method: high-resolution immunofluorescence for the study of the contractile apparatus. *Methods Cell Biol.* 134:573–580.
20. Fukui, Y., T. J. Lynch, H. Brzeska, and E. D. Korn. 1989. Myosin I is located at the leading edges of locomoting *Dictyostelium* amoebae. *Nature (Lond.).* 341:328–331.
21. Gadasi, H., and E. D. Korn. 1980. Evidence for differential intracellular localization of the *Acanthamoeba* myosin isoenzymes. *Nature (Lond.).* 286: 452–456.
22. Hammer, J. A. 1991. Novel myosins. *Trends Cell Biol.* 1:50–56.
23. Hammer, J. A. 1994. The structure and function of unconventional myosins: a review. *J. Muscl. Res. and Cell Motil.* 15:1–10.
24. Harlow, E., and D. Lane. 1988. In: Antibodies. A laboratory manual. Cold Spring Harbor Laboratory, Cold Spring Harbor, NY. 726 pp.
25. Hartwig, J., and D. Kwiatkowski. 1991. Actin binding proteins. *Curr. Opin. Cell Biol.* 3:87–97.
26. Hayden, S. M., J. S. Wolenski, and M. S. Mooseker. 1990. Binding of brush border myosin I to phospholipid vesicles. *J. Cell Biol.* 111:443–451.
27. Jung, G., Y. Fukui, B. Martin, and J. A. Hammer, III. 1993. Sequence, expression pattern, intracellular localization, and targeted disruption of the *Dictyostelium* myosin ID heavy chain isoform. *J. Biol. Chem.* 268:14981–14990.
28. Kulesza-Lipka, D., I. C. Baines, H. Brzeska, and E. D. Korn. 1991. Immunolocalization of myosin I heavy chain kinase in *Acanthamoeba castellanii* and binding of purified kinase to isolated plasma membranes. *J. Cell Biol.* 115:109–119.
29. Kulesza-Lipka, D., H. Brzeska, I. C. Baines, and E. D. Korn. 1993. Autophosphorylation-independent activation of *Acanthamoeba* myosin I heavy chain kinase by plasma membranes. *J. Biol. Chem.* 268:17995–18001.
30. Laemmli, U. K. 1970. Cleavage of structural proteins during the assembly of the head of bacteriophage T4. *Nature (Lond.).* 227:680–685.
31. Lynch, T. J., H. Brzeska, I. C. Baines, and E. D. Korn. 1991. Purification of myosin I and myosin I heavy chain kinase from *Acanthamoeba castellanii*. *Methods Enzymol.* 196:12–23.
32. Maruta, H., and E. D. Korn. 1977. *Acanthamoeba* cofactor protein is a heavy chain kinase required for actin activation of Mg^{2+}-ATPase activity of *Acanthamoeba* myosin I. *J. Biol. Chem.* 252:8329–8332.
33. Mermall, V., J. G. McNally, and K. G. Miller. 1994. Transport of cytoplasmic particles catalyzed by an unconventional myosin in living *Drosophila* embryos. *Nature (Lond.).* 369:560–562.
34. Miyata, H., B. Bowers, and E. D. Korn. 1989. Plasma membrane association of *Acanthamoeba* myosin I. J. Cell Biol. 109:1519–1528.
35. Pollard, T. D., and E. D. Korn. 1973. *Acanthamoeba* myosin. I. Isolation from *Acanthamoeba castellanii* of an enzyme similar to muscle myosin. *J. Biol. Chem.* 248:4682–4690.
36. Rozycki, M. D., J. C. Myslik, C. E. Schutt, and U. Lindberg. 1994. Structural aspects of actin-binding proteins. *Curr. Opin. Cell Biol.* 6:87–95.
37. Titus, M. A. 1993. Myosins. *Curr. Opin. Cell Biol.* 5:77–81.
38. Towbin, H., T. Staehelin, and J. Gordon. 1979. Electrophoretic transfer of proteins from polyacrylamide gels to nitrocellulose sheets: procedure and some applications. *Proc. Natl. Acad. Sci. USA.* 76:4350–4354.
39. Wagner, M. C., B. Barylko, and J. P. Albanesi. 1992. Tissue distribution and subcellular localization of mammalian myosin I. *J. Cell Biol.* 119:163–170.
40. Yonemura, S, and T. P. Pollard. The localization of myosin I and myosin II in *Acanthamoeba* by fluorescence microscopy. 1992. *J. Cell Science.* 102: 629–642.